PHILOSOPHICAL TRANSACTIONS B

Phil. Trans. R. Soc. B.
doi:10.1098/not yet assigned

Exploring nest structures of acorn dwelling ants with x-ray microtomography and surface based 3D visibility graph analysis

Tasos Varoudis[1], Abigail G. Swenson[2], Scott D. Kirkton[3], and James S. Waters[2]

[1] *Bartlett School of Architecture, University College London (UCL), London, UK*
[2] *Department of Biology, Providence College Providence, RI, USA*
[3] *Department of Biological Sciences, Union College, Schenectady, NY, USA*

Keywords: nest architecture, visibility graph analysis, *Temnothorax*, x-rays, microtomography

Main Text

Summary

The physical spaces within which organisms live affect their biology and in many cases can be considered part of their extended phenotype. The nests of social insect societies have a fundamental impact on their ability to function as complex superorganisms. Ants in many species excavate elaborate subterranean nests, but others inhabit relatively small pre-formed cavities within rock crevices and hollow seeds. *Temnothorax* ants, which often nest within acorns, have become a model system for studying collective decision making. While these ants have demonstrated remarkable degrees of rationality and consistent precision with regard to their nest choices, never before has the fine scale internal architecture and spatial organization of their nests been investigated. We used x-ray microtomography to record high resolution 3D scans of *Temnothorax* colonies within their acorns. These data were then quantified using image segmentation and surface based 3D visibility graph analysis (sbVGA), a new computational methodology for analysing spatial structures. The visibility graph analysis method integrates knowledge from the field of architecture with the empirical study of animal-built structures, thus providing the first methodological cross-disciplinary synergy of these two research areas. We found a surprisingly high surface area and degree of spatial heterogeneity within the acorn nests. Specific regions, such as those associated with the locations of queens and brood, were significantly more conducive to connectivity than others. From an architect's point of view, spatial analysis research has never focused on all-surface 3D movement, as we describe within ant nests. Therefore, we believe our approach will provide new methods for understanding both human design and the comparative biology of habitat spaces.

1. Introduction

Visualizing the elaborate and dynamic architecture of social insect nests provides insight into how these societies function [1-4]. Driven by self-organization at the individual worker level, order emerges at the whole-colony level based on interactions between relatively uninformed workers following simple rules in the absence of a leadership hierarchy [5-8]. Examples of emergent order in social insect systems include the division of labour [9], adaptive shape of nest galleries [10,11], and quorum sensing to locate a new nest [12,13]. Architectural elements associated with nests can have impacts on the growth efficiency [14], physiology [15-17], immunity [18-21], and per-capita productivity [22,23]. In order to study the collective

*Authors for correspondence (Tasos Varoudis t.varoudis@ucl.ac.uk and James S. Waters jwaters2@providence.edu).

decision making and building behaviours of these colonies, there are generally two options each with its own strengths and weaknesses. One could examine nest building in a laboratory setting by creating relatively simplified contexts [24-26]; however, this approach neglects the natural habitat and the environment. Alternatively, one could investigate the structure of natural nests; however, this method often requires the destruction of the colony [27-29]. To balance these aims, we investigated the nests of a social insect model system, the acorn-dwelling ants, using x-ray imaging and new analytical methods for studying architectural and social connectivity.

To better understand acorn-dwelling ant nest architecture, we applied computational methodologies commonly used in human architectural analysis. While there are a number of computational analysis methodologies used, one of the most important and widely used is visibility graph analysis (VGA) [30]. VGA analyses the properties of visibility fields by incorporating ideas from space syntax theory [31], early foundation work on visibility fields [32,33], and graph theory [34,35] with details of the visual experience of buildings and urban environments. The concept of the 'isovist' [32], which has had a long history in architecture, geography and mathematics, is central to visibility analysis. An isovist (figure 1) is "the set of all points visible from a given point in space and with respect to the surrounding environment" [32]. Isovists are an intuitively useful way of thinking about a spatial environment because they provide a description of the space 'from inside', a point of view of agents as they perceive, interact, and move through the environment [30].

Until recently, the majority of VGA research was only conducted on a single planar space and with a limited spatial complexity. A recent reformulation of VGA [36,37] incorporated multi-dimensional spatial properties and complex visuospatial relations to create a three dimensional (3D) VGA analysis focused on human habitable spaces (figure 1). In this paper, we apply VGA methods to quantify and better understand the 3D structure and complexity of a social insect nest, the cavity occupied by acorn ants. Ants within these nests may not use vision, but the ray-casting method we developed is relevant to multiple sensory modalities including mechanical and chemo-sensory interactions.

2. Temnothorax x-ray imaging

The nests of many social insect societies can be extensive, housing millions of individuals along with their symbionts and parasites across networks of thousands of interconnected chambers [38]. However, in other cases, smaller colonies may occupy what appear to be much simpler spaces such as the hollow cavities of seeds [39]. As acorns decay and are parasitized, they become hosts to a complex ecosystem of microbial and invertebrate inhabitants, often including whole ant colonies [40]. Mary Talbot described the natural history of acorn ants, remarking on their abundance, their reliance on curculionid beetle larvae having eaten some portion of seed to make a cavity, and suitability for occupation depending on the condition of the acorn with respect to its decay and placement on the forest floor [41,42]. In a recent systematic survey of cavity dwelling ant species in southeastern United States, the inspection of 6,741 nuts from 68 trees revealed 36 species of ants within these cavities, the most common among them being *Temnothorax curvispinosus* [43]. Colonies, ranging in size from queens and a few workers to over 200 individuals, overwinter within the acorns [39,44-46]. Competition for nest sites is influenced by the size of the cavity and believed to shape community structure [47,48]. Consistent with the requirements of their life history, acorn ants have demonstrated consistent geometric preferences in cavity dimensions and the ability to precisely discriminate between alternative nest geometries when given a choice [23,49]. These species also engage in complex house-hunting behaviour, using direct nestmate contact rates to detect a quorum and make decisions in a remarkably rational manner [12,13,50]. Despite their near ubiquity in social insect research, relatively little is known about the architecture and spatial organization of *Temnothorax* within their natural nests.

We collected acorns resting in the forest leaf-litter near Providence College (Rhode Island, USA) that contained live acorn ant colonies (supplemental video S1). To determine that the colony was alive without breaking the acorn open, we searched for worker ants (on average about 2-3 mm long) visible on the forest floor (e.g. foraging or scouting for a new nest). The worker ant was followed back to her nest. Having collected a number of these, we brought the acorns to Union College for x-ray imaging. X-ray imaging is a powerful tool to visualize structure and discover novel biological function in diverse systems ranging from the rhythmic pulsations of insect tracheal systems [51] to the four-dimensional morphology of large vertebrates in locomotion [52]. As a tool for non-destructive morphology, x-ray microtomography has helped

to identify and classify a number of ant species, including ones preserved within amber [53,54], as well as visualize the natural cavities inhabited by small insects [55,56]. Indeed x-ray imaging of artificial ant nest enclosures in the lab has been used to study social insect digging and building behaviours; however, using x-rays to examine these behaviours and the 3D spatial nest organization in natural conditions is technically challenging [28]. Acorn ant colonies should be model systems for this kind of investigation since they offer the advantages of being relatively small and desiccation-resistant, contained within natural cavities, and with low-tempo activity profiles.

Initially, we recorded tomography data using living acorn ant colonies. However, the ants moved in response to the x-ray energy, making image reconstruction impossible. Even the projection-x-ray video in real-time revealed only blurred images as the ants were far more active, due to the x-ray energy, than typically expected for these colonies. As a consequence, we were forced to flash freeze acorns in liquid nitrogen prior to subsequent imaging. The acorns were then warmed to room temperature, wrapped in parafilm, and mounted for scanning in a SkyScan 1272 (Bruker) micro-computed tomography (microCT) system. The acorns were scanned with the x-ray source voltage set to 50.0 kV and the x-ray source current of 200 μA. The best contrast was achieved using a 0.25 mm aluminum filter during the scans. Scans length and resolution varied. One acorn was scanned for over 14 hours at a pixel resolution of 6.08 μm with three x-ray image projections recorded every 0.05 degrees through 180 degrees of rotation. We also scanned two other acorns over 1 hour with a pixel resolution of either 17.0 μm or 19.3 μm. In both cases, x-ray projections were recorded every 0.1 degrees through 180 degrees of resolution. We found that this shorter scan time and resolution was sufficient to analyze the nest cavity architecture and identify the individual ants (figure 2).

The tomographic volumes were reconstructed from projection x-ray images using NRecon software (Bruker). Reconstructions made it possible to clearly visualize the structure of the nest cavity and positions of individual queens, workers, and brood (figure 2 and supplemental movies S1-S3). The reconstructed image stacks were analyzed using CTan (Bruker) to segment the hollow nest cavity and create 3D surface and volume models. Volume data were subsequently visualized using CTVox (Bruker), nest cavity surface areas and volumes were calculated, and 3D shape files describing the nests were exported and used for the surface based 3D visibility graph analysis.

3. Surface based visibility graph analysis

Before introducing the new methodology, we will review the underlying principles of the traditional planar VGA because our proposed approach could abstractly be viewed as a multi-dimensionally warped and convoluted re-imagination of two-dimensional VGA. The new methodology is internally extended through a multi-directional graph representation to work with Euclidean and non-Euclidean spaces **[36,57]**. In early experiments focusing in understanding spatial morphology, the volume of space visible from a location was simplified by taking a horizontal slice (two dimensional) through the isovist polyhedron **[32]**. The resulting isovist is a single polygon (without holes) with calculable geometric properties such as area and perimeter. Through this process, the qualities of space, and their potential, are quantified and compared. When used for the analysis of landscapes, this method provided a 'viewshed' to "[take] away from the architectural space a permanent record of what would otherwise be dependent on either memory or upon an unwieldy number of annotated photographs." **[58]**. In addition, similar ideas have been applied in the field of architecture and planning **[59,60]** and computer generated 'inter-visibility' topographic models **[61]**. A systematic analysis of isovists was performed by Benedikt who believed that analysis of multiple isovists is required to quantify a spatial configuration and suggested that the way through which we experience and use space is related to the interplay of isovists.

Although Benedikt's methods were a leap forward **[32]**, they were somewhat limited as spatial complexity increased. The main limitation is that isovists record only local properties of space, and the visual relationship between the current location and the spatial environment as a whole is not analysed. A second problem was that there was no systematic way to decode the results of the analyses, therefore, there was no framework that connects how isovists relate to spatial, aesthetic or morphological factors. Turner's VGA method combines earlier ideas of morphological analyses using graph theory with space syntax theory and small worlds analysis of networks to produce a graph of mutually visible locations in a spatial layout called 'visibility graph' **[30,62,63]**. The traditional VGA is implemented and widely used by both academics and

practitioners through the open source 'depthmapX' spatial network analysis software **[30,64]**. A number of local and global graph based measures of spatial properties **[65]** can be calculated in depthmapX. In space syntax, the measures can be extracted from the graph and compared with real life data of usage to understand possible morphological or spatial correlations **[66,67]**. More importantly, the local graph measures can be used to understand and describe the shape and complexity of spaces **[68]**.

(a) 2D and 3D VGA

Generating a two-dimensional VGA is a two-step procedure. We first define a set of locations on the plan, which form the vertices of the visibility graph. Next, we employ ray-casting (visibility testing) techniques to construct the graph edges between vertices by expressing the direct visibility relations. The selection and construction of graph vertices is through a grid of locations covering a spatial system at regularly spaced intervals. In VGA, we select an appropriate grid resolution that adequately describes the spatial system with the goal to define a set of locations that offers a near-full description of the space. Moving to three dimensions, a simple 3D VGA analysis method [30] considers all spatial points as nodes in a graph. In particular scenarios, certain points cannot act as locations of activity or spatial importance because all-to-all 3D relations are inherently independent of natural occupancy; however, it can be helpful when investigating pure geometric or morphological relations. In this paper, we focus on a space that is dominated by complex chambers and spatial folds, where occupants can walk along all surfaces and with sensory detection potential for connectivity determined along the lines of the virtual ray-casting.

(b) Surface based 3D VGA analysis

To take advantage of the complexity and detail level that the 3D tomographic process captures, we developed a new method to analyse the morphology of space from within the acorn. The reconstructed tomographic volumes were exported as shape files composed of a triangulated 3D mesh. The surface based 3D visibility graph analysis (sbVGA) begins by subsampling the models to create a set of locations evenly distributed across all surfaces on the nest and to maintain the primary features of the space without excessive resolution that would add unnecessary computation time. As the average distance between subsampled coordinates was approximately 0.25 mm, a distance smaller than an individual ant, we are confident that by erring on the side of relatively abundant detail, nothing was missed in our analysis. For each mesh triangle, the centroid is considered as a possible location. This subset of centroids in space then act as the graph vertices. A ray-casting connectivity check is executed between all pairs of vertices in the graph, establishing an edge if a direct connection exists between two locations in space. These connections and the subsequent 3D hollow 'isovist' represents a spatial graph structure describing the local morphology in a no-ceiling space. Spatial boundaries wrap around the location in question (because ants can move in any direction) and represent a new challenge for spatial analyses. The sbVGA graph is then analysed and selected graph measures are evaluated.

We quantified nest connectivity (or graph degree), closeness centrality (or integration), and local clustering coefficient following Hillier and Hanson's earlier work [31]. The connectivity of a location is equivalent to the degree of the vertex, as discussed in graph theory and represents the number of connections (directly visible locations) that the node has with other nodes in space. Closeness centrality, or integration in classic space syntax literature, is directly linked with 'mean shortest path' of a location to all other locations in the system [30]. Closeness centrality is defined as 1.0 over the sum of all shortest path between the location in question and all other nodes. This gives a statistically similar result to Hillier and Hanson's 'integration'. Mean shortest path is a representation that quantifies the accessibility of every location in a spatial system. If a location in the nest is on average harder to access through edges on the sbVGA graph then its mean shortest path value (or mean depth) will be high. Because mean shortest path or thus closeness centrality measures configuration by considering all locations with respect to each other in the system, global relationships between locations in the system can be explored. In contrast, connectivity and local clustering coefficient is a 'local measure' as it only accounts for the immediate accessible location. Clustering coefficient is defined as the number of connections between all the locations in the neighbourhood of the generating location in question, that is, the number of lines of sight between all the locations forming the isovist, divided by the total number of possible visibility connections with that neighbourhood size [30,62]. In two dimensional isovist terms this is equivalent to finding the mean area of intersection between the generating isovist and all the isovists visible from it, as a proportion of the area of the generating isovist. In our case, the sbVGA gives us a volume consisting of the structural and walkable walls of the nest from each location. Therefore, the measure relates to

the convexity of the 3D volumes, or 3D hollow isovists, at the generating location since sbVGA only considers boundary location and not the empty middle space. If the 3D boundary isovist being considered is a convex volume, then almost all of the point locations within the neighbourhood will be able to see each other and clustering coefficient will tend to 1.0. On the other end of the spectrum, when many points are not visible from each other, meaning the space is very spiky (or maybe has a higher inertia as a volume), clustering coefficients tend towards 0. Clustering coefficient also "indicates how much of an observer's visual field will be retained or lost as one moves away from that point" [30].

4. Results and discussion

Contrary to our prediction and conventional wisdom that acorn ants inhabit relatively hollow spherical cavities, we found that the nests more accurately resembled multiple spaces defined by convoluted and partitioned surfaces, highly compartmentalized architectural elements, and discrete zones of connectivity. The presence of seed remnants, frass, layers of botanical tissue, and multiple topological surfaces contributed to the complexity of these nests. For cavities that measured at their greatest width, 23.7 mm and 25.2 mm diameter spaces, the surface areas and volumes that we actually measured were 1762.5 mm^2 and 770.9 mm^3 for one acorn (nest-101) and 2003.0 mm^2 and 1424.9 mm^3 for a second (nest-103). These measurements average to a surface area to volume ratio of 1.85, a value approximately 460% greater than the predicted ratio expected for simple hollow spherical shaped nest cavities.

Both nests analysed with sbVGA had a closely matched number of graph vertices (node counts), nest-101 has 10,825 analysed locations and nest-103 has 10,952. In space syntax and sbVGA, the comparison of the 'local' measures that describe the immediate surrounding of a location versus a 'global' one like closeness centrality that depicts the morphological relation between the location in question and all other locations helps us understand and quantify the intelligibility of a location, its structural characteristics, and may even expose certain abnormalities [69]. Intelligibility of a space allows us to recognize the global spatial complexity of an arrangement of spaces (or a network of space) by only looking around local space. In highly intelligible environments, orientation and navigation is inherently easier. Intelligibility is a correlation between connectivity and closeness centrality. It indexes the degree to which the number of immediate connections of a location in sbVGA is a reliable guide to the importance of that location in the nest as a whole. A strong correlation, or 'high intelligibility', implies that the whole can be read from the parts. Two main factors are dominant in both nests, the small, compact size and the almost spherical structure with only internal excavations. These features are translated into the balanced scatterplots of connectivity versus closeness and clustering coefficient (figures 3-4).

The distribution of connectivity and closeness values in both nests shows, through the 3D scatterplots (figures 3-4), that while both have a clear inner and outer wall structure, with connectivity values associated with the outer wall as expected (based on the greater range available for ray-casting), nest-103 with its barrel shape generated two distinct peaks in the distributions. The convoluted nature of nest-101 restricts the values of both local and global measures on the bottom part of the nest in favour of the larger chambers at the top. In contrary, the main corridor like structure in nest-103 boosts the closeness centrality values near the two entry points as movement potential through this 'shortcut' is likely.

The queen and brood pile in nest-101 sits in a very interesting location. While the closeness centrality, or mean depth of the area from all other locations, is generally in the middle of the spectrum (all values are normalised between 0.0 and 1.0), local properties of space described by the clustering coefficient depict two adjacent areas where one has a very high value while the other has an extremely low value. In essence, the queen can be relatively accessible by the rest of the nest and also potentially control the level of immediate accessibility very quickly. The area with the low clustering coefficient is one of the areas of the nest that can be seen as top ranked in terms of convexity, it is part of the largest cavity in that nest, so 'openness' and 'control' can be associated with it. The adjacent small chamber has the highest clustering coefficient value and can be seen as the perfect hideout, quickly minimising the distance needed to almost disconnect or hide from the rest of the nest. The distance to the queen's location in comparison to the main nest entrance is one of the longest in the graph, within the top 20% and consistent with a spatial segregation that, in analysis of human dwellings may be associated with a sense of security.

The queen and brood in nest-103 are located at the bottom on the barrel shaped internal structure, seemingly random, but a closer analysis of the depth from the entrance and the structural analysis of the three

total excavated cavities inside the nest give the location a similar character to nest-101. The uniform barrel shape gives the lower part of the nest equivalent graph depth complexity in relation with the entrance at the top. More interesting is that nest-103 has two main internal excavations that are clearly used as 'through movement chambers' allowing inner nest shortcuts, while the queen is located on the opposite side of the nest and segregated from these shortcuts. Based on the local clustering coefficient, the location characteristics depict good local control and some small 'covered' cavities close to the location. Global accessibility to the nest, described by closeness centrality, is uniform because of the barrel structure of the nest.

Unbiased graph-based spatial analyses have never been applied to analyse non-human animal architecture before. The benefits of this approach are 1) the automated and unbiased quantification of configurational relationships with reference to accessibility and other sensory factors, 2) the comparisons from location to location within a system and the ability to compare systems with different geometries, and 3) the relationship of sbVGA measures to manifestations of spatial perception, like movement and space use. The unbiased nature of this approach, based on the uniformly distributed 3D grid used as a basis for modeling nodes and the connectivity calculations, distinguishes it from other network based studies of social insect nest architecture in which nodes and edges within spaces must necessarily be manually identified and classified by the investigator. The major limitation of sbVGA as currently implemented is that the ray-casting connectivity check algorithm used to determine which nodes are connected by edges is not affected by how far apart two nodes may be in space, a factor that may have biological significance depending on the sensory modality for interaction by individuals at these positions. Another limitation concerns the time costs of generating the 3D nest models. We scanned three acorns with ant colonies and a fourth without a colony (see image data presented in figure 2), but only two were used for sbVGA due to constraints primarily associated with the segmentation of the x-ray image data sets.

Although it is not possible to generalize that the architectural features described here are typical for all acorns and other types of nest cavities (e.g. hickory nuts, galls, rock crevices), our work represents a proof of concept with respect to x-ray imaging possibilities, how these data can be quantified using new sbVGA methods, and the potential for future application to habitable spaces in complex structures and novel environments for both humans and animals. Future research that includes more replication, a greater diversity of nest structures, and different null geometric models will further understand how the building and nest-choice behaviours of ants fits into a broader ecological context. For example, the suggestion that acorn ants cultivate and may prefer nests with complex architecture is at least supported by the behaviour observed in lab nests when *Leptothorax tuberointerruptus* workers use sieved sand grains to build partitioning walls around their queen and brood pile [24,25]. Previous studies have demonstrated consistent preferences of *Temnothorax* colonies for nests of certain sizes and proportions [49], but we are unaware of any studies that have subjected these ants to nest choice experiments in which the nest topology varied while potentially holding surface area and/or volume constant. When exposed to potentially stressful stimuli including temperature and microbial growth, *T. curvispinosus* colonies relocated within their acorn, moving larvae toward warmer regions and avoiding microbial contaminants [18]. Since a recent study has demonstrated the successful use of CO_2 anesthesia to temporarily freeze insects for repeated x-ray microtomographic imaging scans [70], their movements and organization behaviors could be visualized at high resolution and tracked within relatively natural nest environments. In addition, the ray-casting method applied here could be modified (e.g. constrained to different scales or types of surface) to match the appropriate sensory modalities and provide a theoretical foundation for understanding how the architecture of inhabited spaces affects the dynamics of human and animal social networks.

Additional Information

Acknowledgments

The authors thank Daniel Higgins and Nicole Korzeniecki from Providence College for their help collecting and working with *Temnothorax* colonies, Alan Penn for his inspiration and feedback on nest morphology and visibility graph modelling, Petros Koutsolampros for helping with the sbVGA video capturing, and the Society for Integrative and Comparative Biology as this research was first noticed by an editor of this issue thanks to a tweet sharing news of our presentation during the poster session of the SICB annual meeting.

Ethics

Research using the invertebrate animals in this study adhered to local guidelines and appropriate ethical standards.

Data Accessibility

We are currently searching for an appropriate database for depositing and sharing the datasets supporting this article.

Authors' Contributions

TV, SDK, and JSW conceived the paper. SDK, AGS, and JSW acquired and analysed x-ray imaging data. TV is responsible for the visibility graph analysis. TV and JSW wrote the final version of the paper with input from all authors.

Competing Interests

We have no competing interests.

Funding

Our use of the micro-computed tomography system at Union College was made possible by a major research instrumentation grant to SDK from the National Science Foundation (DBI-1531850). JSW was supported by a summer research grant from the School of Arts and Sciences at Providence College. TV is supported by UK's Engineering and Physical Sciences Research Council (EPSRC) fund EP/M023583/1.

References

1. Tschinkel, W. R. 2015 The architecture of subterranean ant nests: beauty and mystery underfoot. *Journal of Bioeconomics* **17**, 271–291. (doi:10.1007/s10818-015-9203-6)
2. Moreira, A. A., Forti, L. C., Boaretto, M. A. C., Andrade, A. P. P., Lopes, J. F. S. & Ramos, V. M. 2004 External and internal structure of *Atta bisphaerica* Forel (Hymenoptera: Formicidae) nests. *Journal of Applied Entomology* **128**, 204–211.
3. Seeley, T. D. & Morse, R. A. 1976 The nest of the honey bee (Apis mellifera L.). *Insectes Sociaux* **23**, 495–512. (doi:10.1080/0005772X.1948.11096496)
4. Ocko, S. A., King, H., Andreen, D., Bardunias, P., Turner, J. S., Soar, R. & Mahadevan, L. 2017 Solar-powered ventilation of African termite mounds. *Journal of Experimental Biology* **220**, 3260–3269. (doi:10.1242/jeb.160895)
5. Camazine, S., Deneubourg, J.-L., Franks, N. R., Sneyd, J., Theraulaz, G. & Bonabeau, E. 2003 *Self-organization in biological systems*. Princeton, N.J.: Princeton University Press.
6. Theraulaz, G., Bonabeau, E. & Deneubourg, J. L. 1998 The origin of nest complexity in social insects. *Complexity* **3**, 15-25.
7. Wilson, E. O. & Hölldobler, B. 1988 Dense heterarchies and mass communication as the basis of organization in ant colonies. *Trends Ecol. Evol. (Amst.)* **3**, 65–68.
8. Eom, Y.-H., Perna, A., Fortunato, S., Darrouzet, E., Theraulaz, G. & Jost, C. 2015 Network-based model of the growth of termite nests. *Phys. Rev. E* **92**, 062810. (doi:10.1080/01650520412331333756)
9. Beshers, S. N. & Fewell, J. H. 2001 Models of division of labor in social insects. *Annual Review of Ecology and Systematics* **46**, 413–440.
10. Römer, D. & Roces, F. 2014 Nest Enlargement in Leaf-Cutting Ants: Relocated Brood and Fungus Trigger the Excavation of New Chambers. *PLoS ONE* **9**, e97872. (doi:10.1371/journal.pone.0097872)
11. Bonabeau, E., Theraulaz, G., Deneubourg, J., Franks, N. R., Rafelsberger, O., Joly, J. & Blanco, S. 1998 A model for the emergence of pillars, walls and royal chambers in termite nests. *Philosophical Transactions of the Royal Society B: Biological Sciences* **353**, 1561–1576. (doi:10.1098/rstb.1998.0310)
12. Pratt, S. C., Mallon, E., Sumpter, D. & Franks, N. 2002 Quorum sensing, recruitment, and collective decision-making during colony emigration by the ant *Leptothorax albipennis*. *Behav Ecol Sociobiol* **52**, 117–127. (doi:10.1007/s00265-002-0487-x)
13. Pratt, S. C. 2004 Quorum sensing by encounter rates in the ant *Temnothorax albipennis*. *Behavioral Ecology* **16**, 488–496. (doi:10.1093/beheco/ari020)
14. Brian, M. V. 1953 Brood-rearing in relation to worker number in the ant *Myrmica*. *Physiological Zoology* **26**, 355–366.
15. Cao, T. T. & Dornhaus, A. 2008 Ants under crowded conditions consume more energy. *Biology Letters* **4**, 613–615. (doi:10.1093/beheco/6.3.269)
16. Penick, C. & Tschinkel, W. R. 2008 Thermoregulatory brood transport in the fire ant, *Solenopsis invicta*. *Insectes Sociaux* **55**, 176–182. (doi:10.1007/s00040-008-0987-4)
17. King, H., Ocko, S. & Mahadevan, L. 2015 Termite mounds harness diurnal temperature oscillations for ventilation. *Proceedings of the National Academy of Sciences* **112**, 11589–11593. (doi:10.1073/pnas.1423242112)
18. Karlik, J., Epps, M. J., Dunn, R. R. & Penick, C. A. 2016 Life Inside an Acorn: How Microclimate and Microbes Influence Nest Organization in *Temnothorax* Ants. *Ethology* **122**, 790–797. (doi:10.1111/j.1469-185X.2010.00170.x)
19. Stroeymeyt, N., Pérez, B. C. & Cremer, S. 2014 Organisational immunity in social insects. *Current Opinion in Insect Science* (doi:10.1016/j.cois.2014.09.001)
20. Quevillon, L. E., Hanks, E. M., Bansal, S. & Hughes, D. P. 2015 Social, spatial, and temporal organization in a complex insect society. *Sci Rep* **5**, srep13393. (doi:doi:10.1038/srep13393)
21. Pie, M. R., Rosengaus, R. B. & Traniello, J. F. A. 2004 Nest architecture, activity pattern, worker density and the dynamics of disease transmission in social insects. *Journal of Theoretical Biology* **226**, 45–51. (doi:10.1016/j.jtbi.2003.08.002)
22. Kramer, B. H., Scharf, I. & Foitzik, S. 2013 The role of per-capita productivity in the evolution of small colony sizes in ants. *Behav Ecol Sociobiol* **68**, 41–53. (doi:10.1007/s00265-013-1620-8)
23. Mitrus, S. 2015 The cavity-nest ant Temnothorax crassispinus prefers larger nests. *Insectes Sociaux* **62**, 43–49. (doi:10.1007/s00040-014-0372-4)
24. Franks, N. R., Wilby, A., Silverman, B. W. & Tofts, C. 1992 Self-organizing nest construction in ants: sophisticated building by blind bulldozing. *Animal Behaviour* **44**, 357–375. (doi:10.1016/0003-3472(92)90041-7)
25. Franks, N. & Deneubourg, J. 1997 Self-organizing nest construction in ants: individual worker behaviour and the nest's dynamics. *Animal Behaviour* **54**, 779–796.
26. Downing, H. A. & Jeanne, R. L. 1988 Nest construction by the paper wasp, *Polistes*: a test of stigmergy theory. *Animal Behaviour* **36**, 1729–1739.
27. Perna, A., Jost, C., Couturier, E., Valverde, S., Douady, S. & Theraulaz, G. 2008 The structure of gallery networks in the nests of termite *Cubitermes spp*. revealed by X-ray tomography. *Naturwissenschaften* **95**, 877–884. (doi:10.1673/031.004.2101)
28. Perna, A. & Theraulaz, G. 2017 When social behaviour is moulded in clay: on growth and form of social insect nests. *Journal of Experimental Biology* **220**, 83–91. (doi:10.1242/jeb.143347)
29. Khuong, A., Gautrais, J., Perna, A., Sbaï, C., Combe, M., Kuntz, P., Jost, C. & Theraulaz, G. 2016 Stigmergic construction and topochemical information shape ant nest architecture. *Proceedings of the National Academy of Sciences* **113**, 1303–1308. (doi:10.1073/pnas.1509829113)
30. Turner, A., Doxa, M., O'Sullivan, D. & Penn, A. 2001 From Isovists to Visibility Graphs: a methodology for the analysis of archtiectural space. *Environment and Planning B: Planning and Design* **28**, 103–121.
31. Hillier, B. & Hanson, J. 1984 *The Social Logic of Space*. Cambridge: Cambridge University Press.
32. Benedikt, M. 1979 To take hold of space: Isovist and isovist fields. *Environment and Planning B* **6**, 47–65.
33. Thiel, P. 1961 A sequence experience notation for architectural and urban space. *Town Planning Review* **32**, 33–52.
34. Trudeau, R. J. 1993 *Introduction to Graph Theory*. New York: Dover.
35. Harary, F. 1969 *Graph Theory*. Reading, MA: Addison-Wesley.
36. Varoudis, T. 2014 Augmented Visibility Graph Analysis - Mixed-directionality graph structure for analysing architectural space. In *Fusion - Proceedings of the 32nd eCAADe Conference* (ed E. M. Thompson), pp. 293–302.
37. Varoudis, T. & Psarra, S. 2014 Beyond two dimensions: Architecture through three-dimensional visibility graph analysis. *Journal of Space Syntax* **5**, 91–108.
38. Forti, L., Protti de Andrade, A., Camargo, R., Caldato, N. & Moreira, A. 2017 Discovering the Giant Nest Architecture of Grass-Cutting Ants, *Atta capiguara* (Hymenoptera, Formicidae). *Insects* **8**, 39. (doi:10.1073/pnas.96.14.7998)
39. Headley, A. E. 1943 Population Studies of Two Species of Ants, *Leptothorax longispinosus* Roger and *Leptothorax curvispinosus* Mayr. *Annals of the Entomological Society of America* **36**, 743–753. (doi:10.1093/aesa/36.4.743)
40. Winston, P. W. 1956 The Acorn Microsere, with Special Reference to Arthropods. *Ecology* **37**, 120–132. (doi:10.2307/1929675)
41. Talbot, M. 2012 *The Natural History of the Ants of Michigan's E.S. George Reserve: A 26-year Study*. Ann Arbor: Museum of Zoology, University of Michigan.

42. Talbot, M. 1957 Population Studies of the Slave-Making Ant *Leptothorax duloticus* and Its Slave, *Leptothorax curvispinosus*. *Ecology* **38**, 449–456.
43. Booher, D., Macgown, J. A., HUBBELL, S. P. & Duffield, R. M. 2017 Density and Dispersion of Cavity Dwelling Ant Species in Nuts of Eastern US Forest Floors. *Transactions of the American Entomological Society* **143**, 79–93. (doi:10.3157/061.143.0105)
44. Macgown, J. A. 2006 Hickory Nuts used as Nesting Sites by Ants (Hymenoptera: Formicidae). *Marginalia Insecta* **1**, 1–3.
45. Mitrus, S. 2013 Cost to the cavity-nest ant *Temnothorax crassispinus* (Hymenoptera: Formicidae) of overwintering aboveground. *Eur. J. Entomol.* **110**, 177–179.
46. M Herbers, J. & A Johnson, C. 2007 Social structure and winter survival in acorn ants. *Oikos* **116**, 829–835. (doi:10.1007/BF00379807)
47. Herbers, J. M. & Banschbac, V. 1995 Size-Dependent Nest Site Choice by Cavity-Dwelling Ants. *Psyche: A Journal of Entomology* **102**, 13–17. (doi:10.1155/1995/80574)
48. Foitzik, S. & Heinze, J. 1998 Nest site limitation and colony takeover in the ant *Leptothorax nylanderi*. *Behavioral Ecology* **9**, 367–375. (doi:10.1093/beheco/9.4.367)
49. Pratt, S. C. & Pierce, N. E. 2001 The cavity-dwelling ant Leptothorax curvispinosus uses nest geometry to discriminate between potential homes. *Animal Behaviour* **62**, 281–287. (doi:10.1006/anbe.2001.1777)
50. Sasaki, T. & Pratt, S. C. 2011 Emergence of group rationality from irrational individuals. *Behavioral Ecology* **22**, 276–281. (doi:10.1093/beheco/arq198)
51. Harrison, J. F., Waters, J. S., Cease, A. J., Vandenbrooks, J. M., Callier, V., Klok, C. J., Shaffer, K. & Socha, J. J. 2013 How locusts breathe. *Physiology* **28**, 18–27. (doi:10.1152/physiol.00043.2012)
52. Brainerd, E. L., Baier, D. B., Gatesy, S. M., Hedrick, T. L., Metzger, K. A., Gilbert, S. L. & Crisco, J. J. 2010 X-ray reconstruction of moving morphology (XROMM): precision, accuracy and applications in comparative biomechanics research. *Journal of Experimental Zoology* **313A**, 262–279.
53. Hita Garcia, F., Fischer, G., Liu, C., Audisio, T. L., Alpert, G. D., Fisher, B. L. & Economo, E. P. 2017 X-Ray microtomography for ant taxonomy: An exploration and case study with two new *Teratanер* (Hymenoptera, Formicidae, Myrmicinae) species from Madagascar. *PLoS ONE* **12**, e0172641. (doi:10.1371/journal.pone.0172641)
54. Barden, P., Herhold, H. W. & Grimaldi, D. A. 2017 A new genus of hell ants from the Cretaceous (Hymenoptera: Formicidae: Haidomyrmecini) with a novel head structure. *Syst Entomol* **42**, 837–846. (doi:10.1038/ncomms13658)
55. Farinha, A. O., Branco, M., Pereira, M. F. C., Auger-Rozenberg, M.-A., Maurício, A., Yart, A., Guerreiro, V., Sousa, E. M. R. & Roques, A. 2017 Micro X-ray computed tomography suggests cooperative feeding among adult invasive bugs *Leptoglossus occidentalison* mature seeds of stone pine Pinus pinea. *Agr Forest Entomol* **16**, 281. (doi:10.1146/annurev.ento.49.061802.123329)
56. Aguilera-Olivares, D., Palma-Onetto, V., Flores-Prado, L., Zapata, V. & Niemeyer, H. M. 2017 X-ray computed tomography reveals that intraspecific competition promotes soldier differentiation in a one-piece nesting termite. *Entomologia Experimentalis Et Applicata* **163**, 26–34. (doi:10.1007/BF02223928)
57. Varoudis, T. & Penn, A. 2015 Visibility, accessibility and beyond: Next generation visibility graph analysis. *10th International Space Syntax Symposium*
58. Tandy, C. R. V. 1967 The Isovist Method of Landscpae Survey. In *Symposium: Methods of Landscape Analysis* (ed H. C. Murray), London: Landscape Research Group.
59. Lynch, K. 1976 *What time is this place?* Cambridge: The MIT Press.
60. Amidon, E. L. & Elsner, G. H. 1968 Delineating landscape view areas...a computer approach. *Res Note PSW-RN-180 Berkeley, CA: US Department of Agriculture, Forest Service, Pacific Southwest Forest and Range Experiment Station*
61. Gallagher, G. L. 1972 A computer topographic model for determining intervisibility. In *The Mathematics of Large Scale Simulation* (ed P. Brock), pp. 3–16. La Jolla, CA: Simulation Councils Inc.
62. Watts, D. J. & Strogatz, S. H. 1998 Collective dynamics of 'small-world' networks. *Nature* **339**, 440–442.
63. Ore, O. 1963 *Graphs and their Uses*. New York: Random House.
64. Varoudis, T. 2012 depthmapX – Multi-platform Spatial Network Analyses Software. *github.com*, https:—github.com–varoudis–depthmapX.
65. Brandes, U. & Erlebach, T., editors 2005 *Network Analysis: Methodological Foundations*. Berlin: Springer.
66. Desyllas, J. & Duxbury, E. 2001 Axial Maps and Visibility Graph Analysis. A comparison of their methodology and use in models of urban pedestrian movement. *Proceedings 3rd International Space Syntax Symposium* **27**.
67. Turner, A. & Penn, A. 2002 Encoding natural movement as an agent-based system: an investigation into human pedestrian behaviour in the built environment. *Environment and Planning B: Planning and Design* **29**, 473–490.
68. Psarra, S. & Grajewski, T. 2001 Describing shape and shape complexity using local properties. *Proceedings 3rd International Space Syntax Symposium*, 28–21.
69. Hillier, B., Burdett, R., Peponis, J. & Penn, A. 1987 Creating Life: Or, Does Architecture Determine Anything? *Architecture and Behaviour* **3**, 233–250.
70. Poinapen, D., Konopka, J. K., Umoh, J. U., Norley, C. J. D., McNeil, J. N. & Holdsworth, D. W. 2017 Micro-CT imaging of live insects using carbon dioxide gas-induced hypoxia as anesthetic with minimal impact on certain subsequent life history traits. *BMC Zoology* **2**, 1–13.

Figure and table captions

Figure 1. Spatial analysis and architectural computation. Panel (A) illustrates a traditional method of assessing connectivity, using an isovist to determine the set of all points/locations visible from a given vantage point in space and with respect to the center/starting location. In 3D visibility graph analysis [37], the isovist approach is carried out in three dimensions, comparing the connectedness between all points in space with each other, represented by the color-coded array in panel (B). In panel (C), spatial relations of visibility and accessibility, which in traditional analysis presented challenges, are encoded into a mixed-directionality graph as a way to differentiate the intervisible lines of sight and potential walkable paths between two locations [57]. The surface based graph analysis method we developed and applied in this study builds on the foundation from these earlier approaches to expand spatial analysis to new dimensions and contexts.

Figure 2. Visualizing acorn ant colonies with x-ray microtomography. In the first panel (A), three virtual cross-sections through acorns are shown, with lighter shades of grey associated with higher density plant and animal tissues. The center image shows a cross section including a worker positioned near the nest entrance. The first and third images show a toroidal shape nest cavity surrounding seed tissue in the center. Three dimensional renderings of regions of interest within the scanned acorns are displayed in panels B-E illustrating the density of ants and the complexity of the cavity space within these nests.. Panel F shows a rendering from within one acorn's data set showing a queen *T. curvispinosus* standing over a pile of her larvae. Panel G shows a rendering of a relatively freshly fallen acorn that had not yet been parasitized or occupied by insects.

Figure 3. Surface based 3D visibility graph analysis (sbVGA) of nest-101. Panels A-B show the surface points used in the analysis color-coded by connectivity (graph vertex degree) separated by a 230° rotation. Panels C-D show the analysed surface points color-coded by local clustering coefficient, separated by a 230° rotation. Asterisks indicate approximate locations of the queen and brood pile. Panels E and F plot connectivity, as a description of local properties of space, against closeness centrality and clustering coefficient.

Figure 4. Surface based 3D visibility graph analysis (sbVGA) of nest-103. Panels A-B show the surface points used in the analysis color-coded by connectivity (graph vertex degree) separated by a 230° rotation. Panels C-D show the analysed surface points color-coded by local clustering coefficient, separated by a 230° rotation. Asterisks indicate approximate locations of the queen and brood pile. Panels E and F plot connectivity, as a description of local properties of space, against closeness centrality and clustering coefficient.

Figure 1

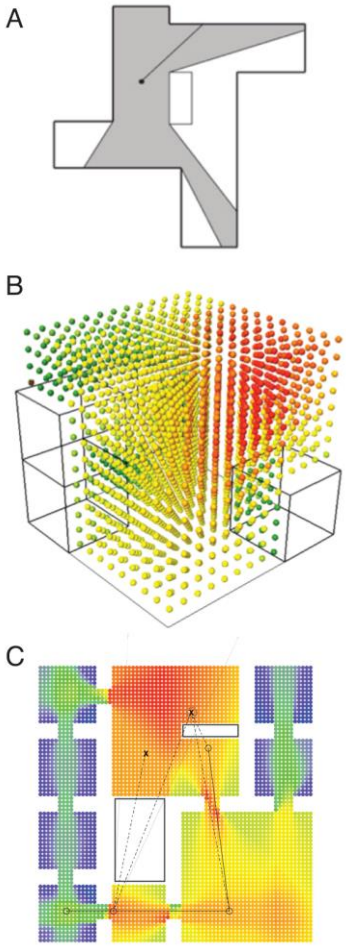

Figure 1. Spatial analysis and architectural computation. Panel (A) illustrates a traditional method of assessing connectivity, using an isovist to determine the set of all points/locations visible from a given vantage point in space and with respect to the center/starting location. In 3D visibility graph analysis [37], the isovist approach is carried out in three dimensions, comparing the connectedness between all points in space with each other, represented by the color-coded array in panel (B). In panel (C), spatial relations of visibility and accessibility, which in traditional analysis presented challenges, are encoded into a mixed-directionality graph as a way to differentiate the intervisible lines of sight and potential walkable paths between two locations [57]. The surface based graph analysis method we developed and applied in this study builds on the foundation from these earlier approaches to expand spatial analysis to new dimensions and contexts.

Figure 2

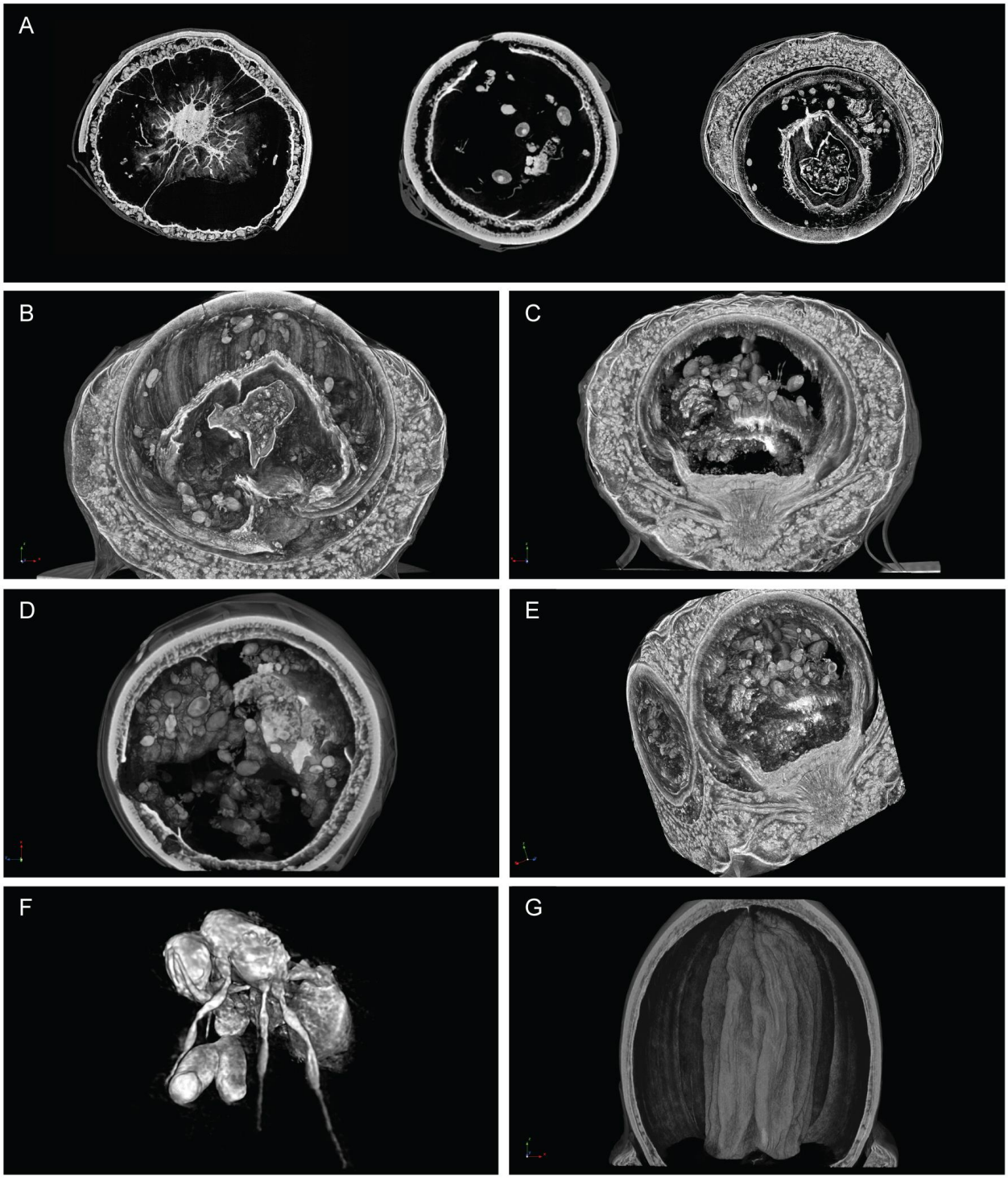

Figure 2. Visualizing acorn ant colonies with x-ray microtomography. In the first panel (A), three virtual cross-sections through acorns are shown, with lighter shades of grey associated with higher density plant and animal tissues. The centre image shows a cross section including a worker positioned near the nest entrance. The first and third images show a black toroid shaped nest cavity surrounding seed tissue in the centre. Three dimensional renderings of regions of interest within the scanned acorns are displayed in panels B-E illustrating the density of ants and the complexity of the cavity space within these nests.. Panel F shows a rendering from within one acorn's data set showing a queen *T. curvispinosus* standing over a pile of her larvae. Panel G shows a rendering of a relatively freshly fallen acorn that had not yet been parasitized or occupied by insects.

Figure 3

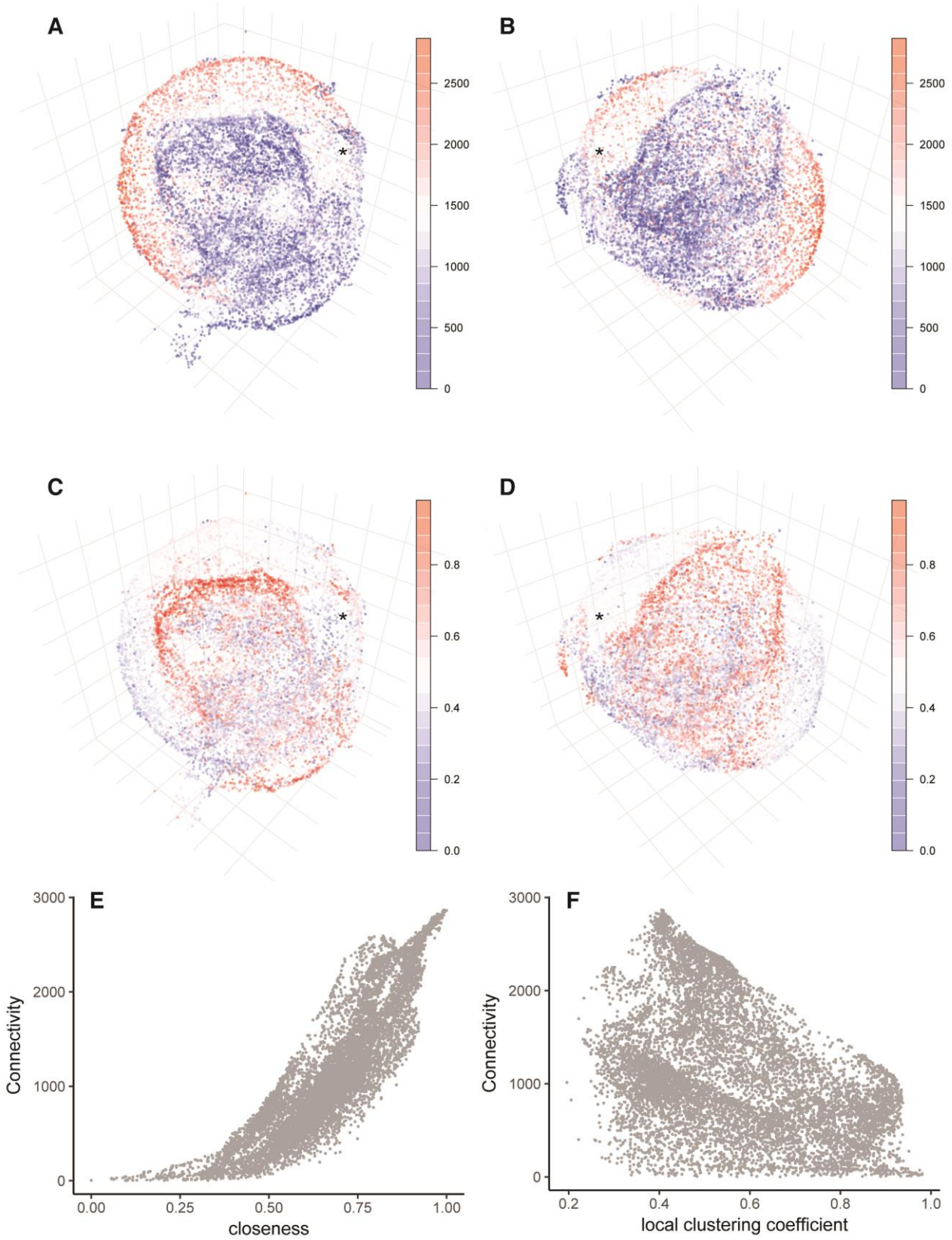

Figure 3. Surface based 3D visibility graph analysis (sbVGA) of nest-101. Panels A-B show the surface points used in the analysis color-coded by connectivity (graph vertex degree) separated by a 230° rotation. Panels C-D show the analysed surface points color-coded by local clustering coefficient, separated by a 230° rotation. Asterisks indicate approximate locations of the queen and brood pile. Panels E and F plot connectivity, as a description of local properties of space, against closeness centrality and clustering coefficient.

Figure 3

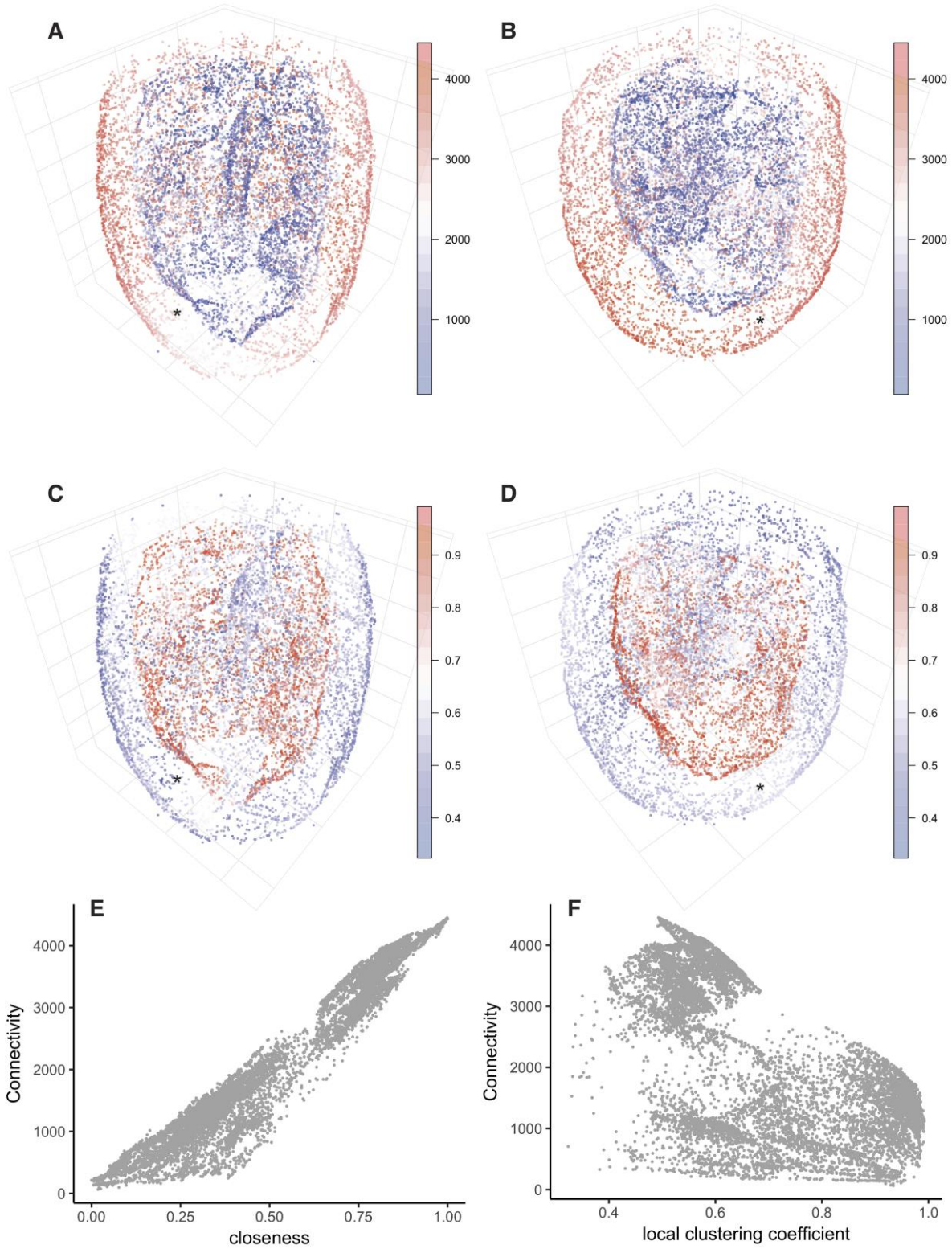

Figure 4. Surface based 3D visibility graph analysis (sbVGA) of nest-103. Panels A-B show the surface points used in the analysis color-coded by connectivity (graph vertex degree) separated by a 230° rotation. Panels C-D show the analysed surface points color-coded by local clustering coefficient, separated by a 230° rotation. Asterisks indicate approximate locations of the queen and brood pile. Panels E and F plot connectivity, as a description of local properties of space, against closeness centrality and clustering coefficient.

Supplementary material

Movie S1. Video of a *Temnothorax curvispinosus* worker exiting her colony's nest on the forest floor, walking around, encountering other ants, and returning to her acorn. The video (54 s, 30 fps) was recorded using an iPhone after manually searching the forest floor to locate foraging individuals and acorns with small openings that may have contained colonies within. Acorns such as this one were collected (without breaking them open for inspection) and promptly used for the x-ray imaging reported in this study.

Movie S2. Video showing sequential slices in a 3D image stack generated by x-ray microCT imaging of an acorn ant nest containing a colony of *Temnothorax curvispinosus*.

Movie S3. Video showing a 3D rendering of an acorn ant nest and a virtual flight into the cavity, revealing the complexity of internal structure and clarity of resolving individual ants.

Movie S4. Video showing a progressive 3D point cloud generation color-coded with sbVGA connectivity values of nest-101, demonstrating the complex internal structure and the distribution of values inside the convoluted cavities.

Movie S5. Video showing a progressive 3D point cloud generation color-coded with sbVGA connectivity values of nest-103, demonstrating the complex internal structure and the distribution of values inside the convoluted cavities.